International Journal of Mass Spectrometry 283 (2009) 135–139

Contents lists available at ScienceDirect

International Journal of Mass Spectrometry

journal homepage: www.elsevier.com/locate/ijms

Infrared spectroscopy of gas-phase hydrated K^+:18-crown-6 complexes: Evidence for high energy conformer trapping using the argon tagging method

Jason D. Rodriguez, James M. Lisy*

Department of Chemistry, University of Illinois at Urbana-Champaign, Urbana, IL 61801, United States

ARTICLE INFO

Article history:
Received 3 December 2008
Received in revised form 24 February 2009
Accepted 25 February 2009
Available online 24 March 2009

Keywords:
Crown ethers
Argon tagging
Conformer trapping
Vibrational spectroscopy

ABSTRACT

We report our findings on the K^+(18-crown-6 ether)$(H_2O)_1Ar_{1-4}$ system using gas-phase infrared predissociation (IRPD) spectroscopy. With the argon tagging technique, we have been able to observe two different conformers, including a conformer that features a bidentate H_2O actively competing with K^+ for the preferred binding site inside the 18-crown-6 cavity. The detection of this conformer in our experiment was surprising since density functional theory (DFT) calculations predict it to be 55.6 kJ mol^{-1} higher in energy than the lower energy, traditional (K^+ bound)-type conformer. We have been able to selectively probe each conformer by varying both the loss channel monitored and the number of solvating argons. The bidentate conformer was present in the IRPD spectra only when monitoring the action spectrum leading to the loss of all ligands. This suggests that the bidentate conformer undergoes rearrangement following photoexcitation to the much more stable bare K^+(18-crown-6) complex. We explored the barrier to such rearrangement using D_2O substitution in the experiment and with DFT calculations.

1. Introduction

Ionophore-model systems, such as crown ethers, have attracted much attention due to their versatility in many applications. Recently, crown ethers have been used in molecular wires [1], in applications dealing with organic electrides [2], and as stabilizers of ionic compounds used to study aromaticity [3]. One of the most studied crown ethers, 18-crown-6 ether (18c6), has been shown to selectively bind K^+ in aqueous solution [4]. This special affinity in the condensed-phase has been attributed to a variety of factors including the "best-fit" phenomena [5] between K^+ and the 18c6 cavity. However, initial gas phase studies [6,7] of alkali metal ion:18c6 complexes did not replicate this selective behavior of 18c6 for K^+. Experimental [8,9] and computational [10] studies showed that the effect of microhydration was crucial in bridging the gap between the gas phase and the condensed phase. Using gas-phase infrared predissociation (IRPD) spectroscopic techniques, we report our results on the singly hydrated K^+(18c6) system (H_2O and D_2O) at the molecular level.

We have incorporated the Ar tagging technique [11] in the generation of these species to produce colder complexes with less internal energy [12], and thus better resolved spectral features. Surprisingly, this technique has also allowed us to trap out a high energy stable species that is much higher in energy (55.6 kJ mol^{-1}) compared to the minimum energy conformer predicted by density functional theory (DFT). This conformer, upon irradiation with an IR photon, dissipates significant amounts of energy leading to loss of all ligands up to the bare, unsolvated K^+(18c6) complex and is present in the IRPD spectra only when monitoring the loss of $Ar_m + H_2O$. This is different from previous work with Ar tagged complexes, where the IR action spectra are primarily acquired by monitoring the loss of the weakly bound Ar messenger atom.

2. Experimental

A complete description of the experimental apparatus has been reported elsewhere [13], so only a brief overview will be presented here. A mixture of Ar carrier gas seeded with H_2O is passed over a heated sample holder (90–100 °C) containing crystalline 18c6. The resulting 18c6/H_2O/Ar gas mixture is allowed to fully expand forming neutral clusters before colliding with K^+ ejected via thermionic emission from a tungsten filament. Nascent cluster ions stabilize via evaporative cooling and enter the detector chamber via a 2.0 mm skimmer. Cluster ions are guided with an octapole ion guide and a stack of electrostatic lenses to the triple quadrupole mass spectrometer portion the apparatus. The parent cluster ions of interest are mass selected in the first quadrupole. These mass selected clusters then enter the second quadrupole (rf-only), which serves as an ion guiding quadrupole. While in the second quadrupole, the cluster ions interact with the output of a tunable IR laser (Laser Vision OPO/OPA pumped by a 10 Hz Nd:YAG laser). Fragment ions of interest are mass-analyzed by the third quadrupole and the action

* Corresponding author. Tel.: +1 217 333 2898; fax: +1 217 244 3186.
E-mail address: j-lisy@uiuc.edu (J.M. Lisy).

1387-3806/$ – see front matter © 2009 Elsevier B.V. All rights reserved.
doi:10.1016/j.ijms.2009.02.029

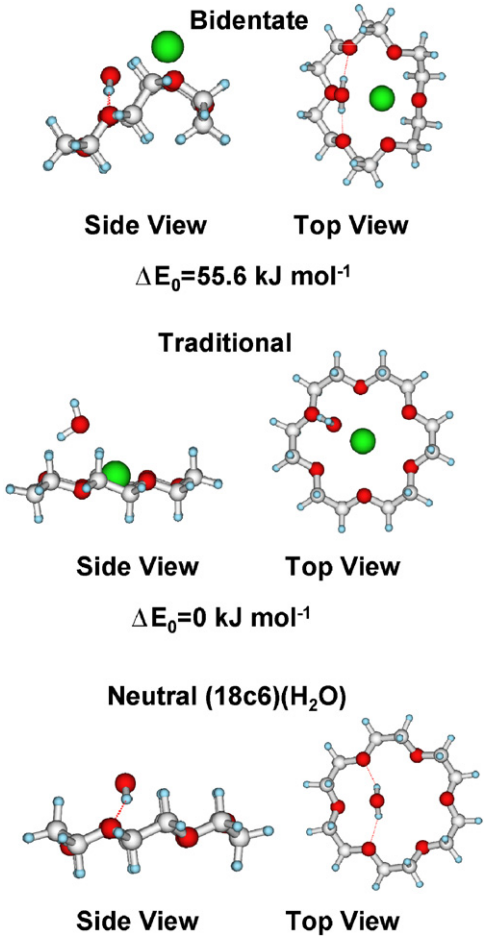

Fig. 1. The calculated DFT (B3LYP/6-31 + G*) structures of the two conformers found for K^+(18c6)(H_2O): bidentate (B) and traditional (T). The neutral 18c6(H_2O) is also shown.

spectrum is recorded as a function of laser frequency. A three-point averaging procedure was applied to smooth the experimental spectra.

3. Calculations

We performed DFT calculations (B3LYP/6-31 + G*) on the singly hydrated K^+(18c6) system (H_2O and D_2O) using Gaussian 03 [14]. Further calculation details are available in supporting information section. Previous theoretical work [15] indicates that there are three low lying conformations for 18c6(H_2O), two of which feature single hydrogen bonds and one with a bidentate hydrogen-bonded water. In K^+(18c6)(H_2O), previous *ab initio* calculations by Feller [10] indicate that the most favored configuration features K^+ nestled inside the 18c6 cavity with H_2O coordinated to K^+ and forming a hydrogen bond with one 18c6 oxygen. The only two stable K^+(18c6)(H_2O) conformers found in this study are shown in Fig. 1. The Ar atoms are not shown in the structures, but have been included in the calculations of zero point binding energies, discussed later. The traditional (T) conformer is similar to the structure reported by Feller, while the bidentate (B) conformer is higher in energy by 55.6 kJ mol^{-1} with respect to the T conformer and owes its name to the bidentate (or double donor) hydrogen bonding orientation of H_2O in the complex. Unlike the T conformer, which features a near-planar configuration of 18c6, the B conformer is highly distorted due to the orientation of the bidentate H_2O and the off-center site occupied by K^+ above the 18c6 cavity. We also attempted to find similar structures with backside (on opposite side of K^+) H_2O binding, but geometry optimizations quickly converged to the T conformer.

4. Results and discussion

The experimental IRPD spectra and calculated spectra based on the scaled harmonic vibrational frequencies are shown in Fig. 2. The experimental spectra were acquired in the 2600–3800 cm^{-1} region monitoring either the loss of Ar_m or loss of $Ar_m + H_2O$. In the OH stretching region, 3100–3800 cm^{-1}, there are stark differences between the spectra acquired monitoring the loss of Ar_m and those acquired monitoring the loss of $Ar_m + H_2O$. The spectra acquired monitoring the loss of Ar_m are shown in panel (A). For $m = 1$, there are two features, a hydrogen-bonded feature located at ~3579 cm^{-1} and a free OH stretch located at ~3725 cm^{-1}. In $K^+(H_2O)Ar$, which exhibits no hydrogen bonding, the symmetric and asymmetric OH stretches were observed [16] at 3636 and 3710 cm^{-1}, respectively. While the free OH feature is constant through the entire $m = 1$–4 progression, there are slight changes in the hydrogen-bonded feature. Starting at $m = 2$ a second, lower frequency peak appears at ~3566 cm^{-1}, giving the hydrogen-bonded feature a broader appearance. The higher (~3579 cm^{-1}) frequency band diminishes in relative intensity with each subsequent addition of Ar and by $m = 4$, the lower frequency band is the more dominant hydrogen-bonded feature with the higher frequency peak occurring as a shoulder.

The spectra acquired monitoring the loss of $Ar_m + H_2O$ are shown in panel (B). These spectra are more complex than the loss of Ar_m spectra and change substantially with each stepwise addition of Ar. In $m = 1$ there are three hydrogen-bonded OH features located at 3516, 3560, and 3576 cm^{-1}, and a free OH feature located at 3725 cm^{-1}. The peaks at 3576 and 3725 cm^{-1} are nearly identical to those appearing in the Ar_1 loss channel, but with each additional Ar they are further suppressed. Starting at $m = 2$, the features at 3516 and 3560 cm^{-1} are the most prominent OH transitions.

In the CH stretching region, 2600–3100 cm^{-1}, the differences between the loss of Ar_m and loss of $Ar_m + H_2O$ channels are more subtle than in the OH stretching region. Both loss channels have a series of sharp bands in the 2875–2950 cm^{-1} region. The position of these features agrees well with the symmetric and asymmetric stretches of gas-phase neutral 18c6, which has symmetric and asymmetric stretches at ~2870 and 2920 cm^{-1}, respectively [17]. The areas where the loss channels are clearly different are in the spectral region surrounding symmetric and asymmetric stretches. In the loss of Ar_m spectra, there are various weak transitions in the region below 2875 cm^{-1}, while in the loss of $Ar_m + H_2O$ spectra there are no discernable features. In the region above 3000 cm^{-1}, there appear to be two peaks in the loss of Ar_m spectra while there are three distinguishable peaks in the loss of $Ar_m + H_2O$ for $m = 1$–3. In the loss of $Ar_4 + H_2O$ spectrum, it is difficult to resolve these peaks because the relative intensity of the CH stretching region as compared to the OH stretching region is noticeably lower. This indicates that the decreased photon energy in this region is reducing the quantum yield in the loss of $Ar_m + H_2O$ channel. Such a trend is important because it suggests that there may be a minimum energy threshold to keep the $Ar_m + H_2O$ loss channel active. This behavior is not observed in the Ar_m loss channel.

Comparison of the calculated spectra for the two possible conformers, T and B, shows that T conformer is the only conformer present in the spectra when monitoring the loss of Ar_m, while B is the dominant conformer detected when monitoring the loss of $Ar_m + H_2O$. The slight change in the hydrogen-bonded OH stretch in Fig. 2A, may be a small secondary effect arising from the addition of a second (or more) argon(s). It does not lead to any other significant change in the spectra. In the loss of $Ar_1 + H_2O$ spectrum, discussed

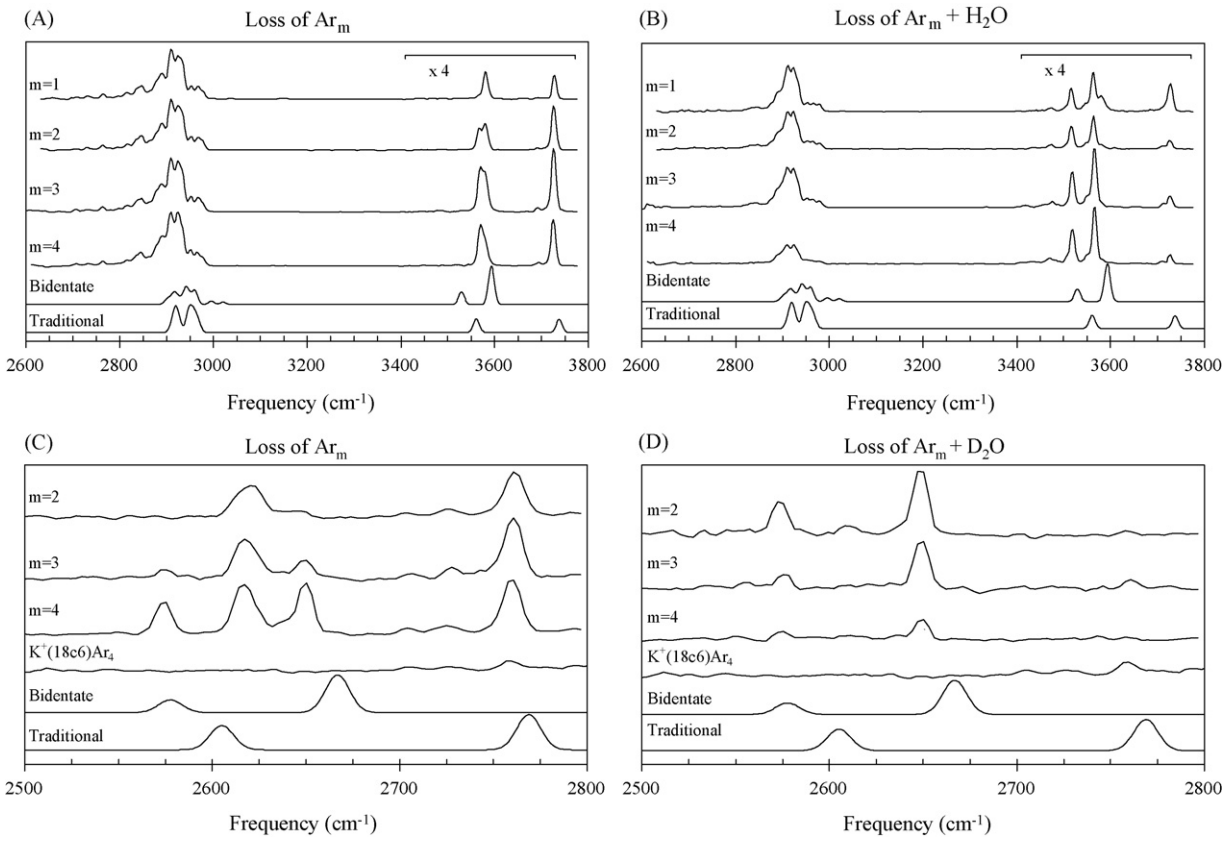

Fig. 2. The experimental spectra for $K^+(18c6)(H_2O)Ar_m$ and $K^+(18c6)(D_2O)$ Ar_m complexes acquired by monitoring different loss channels: (A) H_2O:Loss of Ar_m (B) H_2O:Loss of $Ar_m + H_2O$ (C) D_2O:Loss of Ar_m and (D) D_2O:Loss of $Ar_m + D_2O$. The calculated spectra are also shown for traditional (T) and bidentate (B) conformers based on the DFT harmonic vibrational frequency calculations (B3LYP/6-31 + G*). The experimental spectra are enhanced (×4) in the OH stretching region. The simulated spectra correspond to the calculations not including the Ar atoms.

earlier, there does seem to be a coexistence of both conformers. However with each stepwise addition of Ar, the changes are significant; the B conformer becomes the dominant conformer sampled in our experiment. Previous studies in our group on hydrated alkali metal ion systems [18] have shown that the argon evaporation method allows low energy configurations of the neutral clusters to interact with the approaching ion. Rapid argon evaporation effectively dissipates the kinetic energy, leaving the resulting complexes with very low internal energies and, in some cases, in non-global minimum energy conformations. The low internal energies limit the degree to which these species can surmount barriers to rearrangement to lower energy structures, and thus higher energy conformers may be trapped. This seems to be the case in the B conformer where the neutral bidentate $(18c6)H_2O$, mentioned earlier [15] as one of the preferred configurations for the monohydrated neutral system, may first be formed in the argon cluster with a sufficient barrier for K^+ to replace the bidentate H_2O inside the 18c6 cavity. We performed DFT calculations on the neutral $(18c6)H_2O$ system to gain insight on the B conformer, since the aforementioned hydrated alkali metal ion systems [18] showed that the high energy conformers, trapped in our previous experiments, mirror robust neutral structures that failed to undergo rearrangement after ion impact. The minimum energy structure of neutral $(18c6)H_2O$, shown in Fig. 1, features H_2O bound to 18c6 cavity via a bidentate hydrogen bond, similar to the B conformer. This indicates that the structure of the B conformer is strongly influenced by "freezing" the neutral $(18c6)H_2O$ complex. The calculated frequencies of the two hydrogen-bonded OH vibrations in $(18c6)H_2O$ are at 3593 and 3680 cm^{-1} and are the symmetric and asymmetric stretching modes. The 87 cm^{-1} splitting in the $(18c6)H_2O$ complex is roughly twice the splitting of the two bidentate hydrogen bonds in the B conformer observed experimentally at 3516 and 3560 cm^{-1}, in the loss of $Ar_m + H_2O$ spectra. In recent spectroscopic studies on hydrated 18c6 derivatives [19,20], where H_2O was also bound to the 18c6 moiety via a bidentate hydrogen bond, the symmetric and asymmetric splitting was found to be ~68–83 cm^{-1}.

The ability to lose H_2O and multiple Ar atoms in these complexes is surprising. The photoexcitation of either of the bidentate hydrogen bonds in the B conformer sets in motion a sequence of events that ultimately leads to the dissipation of the excess energy via sequential loss of all of the ligands. We are able to detect this sequence only in the loss of $Ar_m + H_2O$ channel. Although future efforts will be made to better understand the exact mechanism in which these high energy complexes undergo to lose all their ligands, we attempted to qualitatively assess whether there is a minimum photon energy required to set this process in motion by using D_2O. Panels (C) and (D) in Fig. 2 show our experimental results in the OD stretching region, 2500-2800 cm^{-1}, and corresponding calculated spectra for $K^+(18c6)(D_2O)Ar_{m=2-4}$. In each case we have included $K^+(18c6)Ar_4$ as a reference spectrum to account for any transitions not associated with D_2O. Mass overlap with $K^+(18c6)(D_2O)_3$ precluded acquiring the spectrum of the $m = 1$ species in the D_2O studies. The loss of Ar_2 spectrum in panel (C) shows a profile very similar to that observed in the H_2O loss of Ar_m spectra, with a lone hydrogen-bonded OD and a free OD stretch at 2620 and 2761 cm^{-1}, respectively. The frequency splitting in the OD vibrations (141 cm^{-1}) is remarkably consistent with that observed for the OH vibrations (146 cm^{-1}). Starting at $m = 3$ and prominently in $m = 4$, there are four features. The features at 2572, 2617, and 2650 cm^{-1} are due to OD hydrogen-bonded OD stretching bands,

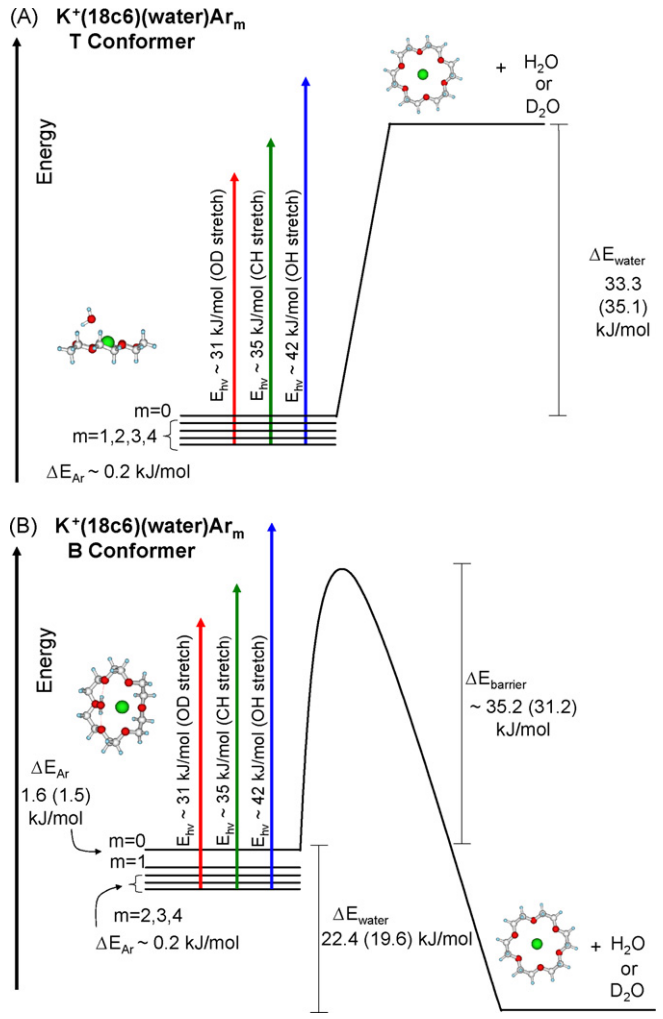

Fig. 3. (A) Binding energy diagram for the (T) conformer. (B) Rearrangement of the bidentate (B) structure to the lower energy unsolvated (T)-type structure following photoexcitation. In both (A) and (B) the zero-point binding energies (ZPBE) (in kJ mol^{-1}) were calculated from the DFT harmonic vibrational frequency calculations (B3LYP/6-31 + G*) and are given for Ar and H_2O (D_2O in parentheses).

while the feature at 2758 cm^{-1} is due to the free OD stretch. In the loss of $Ar_m + D_2O$ spectra, panel (D), only $m = 2$ has significant IR photodissociation intensity with two peaks, both hydrogen-bonded OD stretches at 2572 and 2650 cm^{-1}. These peaks are due to the bidentate D_2O hydrogen bonds in the B-type structure, where once again, there is strong consistency between the D_2O and H_2O systems with splittings of 45 and 44 cm^{-1}, respectively. This loss channel is effectively quenched starting at $m = 3$ and the features are transferred to the Ar_m loss channel. In the Ar_m loss channel, there is initially only the T conformer present in the experiment for $m = 2$ and a combination of both T and B for $m = 3, 4$.

Two energy diagrams to help illustrate the photodissociation dynamics, reported for both the T and B conformers, are shown in Fig. 3. The zero-point binding energies (ZPBE) were calculated using the B3LYP/6-31 + G* harmonic vibrational frequency calculations. The photon energy ($E_{h\nu}$) for each of the three regions scanned experimentally (OD, CH and OH stretches) is also shown in Fig. 3. As can be seen for the T conformer in Fig. 3A, excitation of the OH stretch has sufficient energy ($E_{h\nu}$ ~42 kJ mol^{-1}) to induce the loss of H_2O (ZPBE 33.3 kJ mol^{-1}) and Ar (ZPBE ~0.2 kJ mol^{-1}) for $K^+(18c6)(H_2O)Ar$ leading to the appearance of the T conformer in the $Ar_1 + H_2O$ loss channel. However, with each subsequent Ar added to the system, less excess energy is left for the H_2O and Ar_m to evaporate, essentially causing the IR signature hydrogen-bonded OH stretch at 3576 cm^{-1} of the T conformer to vanish from the $Ar_m + H_2O$ loss channel. The free OH stretch at ~3725 cm^{-1} remains, although much weaker. This may be due to the slightly greater photon energy which can facilitate the $Ar_m + H_2O$ loss. In the CH stretching region, the photon energy ($E_{h\nu}$ ~ 35 kJ mol^{-1}) is insufficient to dissociate both H_2O and Ar for the T conformer so the features appearing below 3000 cm^{-1} in the $Ar_m + H_2O$ loss channel in Fig. 2B are all due to conformer B. In the D_2O-containing complexes the main determining factor of the features observed, when monitoring the different loss channels, is the photon energy in the OD stretching region. In this region there is only enough energy for the T conformers to lose Ar_m since the binding energy of D_2O (ZPBE 35.1 kJ mol^{-1}) exceeds the photon energy ($E_{h\nu}$ ~31 kJ mol^{-1}).

The B conformer is never observed in the loss of Ar_m channel in the OH stretching region. This is because once any of the bidentate OH bands are excited, a chain of events is started allowing a rearrangement to take place, likely driven by K^+ shifting into a more energetically stable location in the center of the 18c6 cavity. The available energy resulting from this rearrangement (photon + B→T) is much greater than the collective binding energy of the argons (ZPBE 1.6 kJ mol^{-1} for the first argon and ~0.2 kJ mol^{-1} for the subsequent argons) and H_2O (ZPBE 22.4 kJ mol^{-1}), with the resulting complex being the extremely stable $K^+(18c6)$ as depicted in Fig. 3B. In the D_2O-containing complexes, the B conformer also behaves the same as in H_2O for $m = 2$ and to a lesser extent for $m = 3$, as seen in Fig. 2D with the loss of Ar_m and H_2O. However, something interesting happens at $m = 4$. Almost no signal is observed in the $Ar_4 + H_2O$ loss channel. Instead both B and T conformers are present in the Ar_4 loss channel. The B conformer appears in this channel because the energy of the photon is insufficient to surmount the barrier that starts the rearrangement process. The only channel that remains open is the one where the excess energy is dissipated through the loss of all four Ar atoms. This clearly indicates that the energy diagram for the B conformer in Fig. 3B is quite different from that for the T conformer; there is a substantial energy barrier for the rearrangement to take place.

The existence of this barrier is also supported by results from the H_2O-containing systems; the $Ar_m + H_2O$ loss channel is significantly suppressed in the CH stretching region starting at $m = 4$. Based on these observations, we can obtain an experimental estimate for the barrier height for the rearrangement to be ~35.2 kJ mol^{-1}, which corresponds to the center of the CH stretching region plus the estimated energy of binding the fourth Ar. In the D_2O-containing system, the B structure fails to undergo rearrangement at $m = 4$, and we can estimate the barrier height for the rearrangement to be ~31.2 kJ mol^{-1}, which is the photon energy in the center of the OD region plus the estimated binding energy of the fourth Ar. The difference between these two values may reflect the efficiency in different vibrational modes to surmount the barrier. In the bidentate structure, the OD stretches will likely couple more directly to the coordinate that converts the B to the T conformer. The CH stretches will couple into the 18c6 ring modes which may not be as effective in displacing the water in the B conformer. Using these estimated barrier heights from experiment, the energy diagram for the B conformer is shown in Fig. 3B. As the photon energy ($E_{h\nu}$) is decreased, the likelihood of overcoming the barrier to rearrangement is diminished and this is seen experimentally as a reduction in quantum yield in the Ar_4+ H_2O loss channel in the CH stretching region and deactivation of the $Ar_4 + D_2O$ loss channel in the OD stretching region.

5. Conclusions

The IRPD spectra of two different $K^+(18c6)(H_2O)Ar_{1-4}$ conformers have been obtained using the argon tagging technique. One of

these conformers is a high energy structure that features H_2O in a bidentate hydrogen-bonded orientation, the other is the traditional structure with the K^+ centered in the 18c6 with the water directly above the ion. Stepwise addition of Ar and the monitoring of different loss channels to acquire the action spectra have allowed us to selectively probe each species. Upon photoexcitation, the high energy structure, B, undergoes rearrangement that leads to the loss of water and all argons, leaving the K^+(18c6) complex. Consequently, this conformer can only be detected only in the $Ar_m + H_2O$ loss channel. Experiments using D_2O have shown that photon energy plays a critical role, and there is a substantial barrier with a minimum energy of $\sim$31.2 kJ mol^{-1} required to drive the rearrangement process. We intend to further examine and exploit the ability to trap high energy conformers to map the potential energy surfaces of these and other strongly bound non-covalent complexes.

Acknowledgements

The authors wish to thank the National Science Foundation (Grants CHE-0415859, CHE-0748874, and CRIF-0541659) for partial support of this research. Computational work was done on NCSA Cobalt Supercomputer System (Award no. TG-CHE070097).

Appendix A. Supplementary data

Supplementary data associated with this article can be found, in the online version, at doi:10.1016/j.ijms.2009.02.029.

References

[1] C. Liu, D. Walter, D. Neuhauser, R. Baer, J. Am. Chem. Soc. 125 (2003) 13936–13937.
[2] J.L. Dye, Science 301 (2003) 607–608.
[3] A. Ugrinov, A. Sen, A.C. Reber, M. Qian, S.N. Khana, J. Am. Chem. Soc. 130 (2008) 782–783.
[4] R.M. Izatt, J.H. Rytting, D.P. Nelson, B.L. Haymore, J.J. Christensen, Science 164 (1969) 443–444.
[5] J.J. Christensen, J.O. Hill, R.M. Izatt, Science 174 (1971) 459–467.
[6] J.S. Brodbelt, C.-C Liou, Pure Appl. Chem. 65 (1993) 409–414.
[7] D.V. Dearden, H. Zhang, I.H. Chu, P. Wong, Q. Chen, Pure Appl. Chem. 65 (1993) 423–428.
[8] M.B. More, D. Ray, P.B. Armentrout, J. Am. Chem. Soc. 121 (1999) 417–423.
[9] P.B. Armentrout, Int. J. Mass spectrom. 193 (1999) 227.
[10] D. Feller, J. Phys. Chem. A 101 (1997) 2723–2731.
[11] W.H. Robertson, E.G. Diken, E.A. Price, J.-W. Shin, M.A. Johnson, Science 299 (2003) 1367–1372.
[12] C.E. Klots, J. Chem. Phys. 83 (1985) 5854–5860.
[13] J.M. Lisy, Int. Rev. Phys. Chem. 16 (1997) 267–289.
[14] M.J. Frisch, G.W. Trucks, H.B. Schlegel, G.E. Scuseria, M.A. Robb, J.R. Cheeseman, J.A. Montgomery Jr., T. Vreven, K.N. Kudin, J.C. Burant, J.M. Millam, S.S. Iyengar, J. Tomasi, V. Barone, B. Mennucci, M. Cossi, G. Scalmani, N. Rega, G.A. Petersson, H. Nakatsuji, M. Hada, M. Ehara, K. Toyota, R. Fukuda, J. Hasegawa, M. Ishida, T. Nakajima, Y. Honda, O. Kitao, H. Nakai, M. Klene, X. Li, J.E. Knox, H.P. Hratchian, J.B. Cross, C. Adamo, J. Jaramillo, R. Gomperts, R.E. Stratmann, O. Yazyev, A.J. Austin, R. Cammi, C. Pomelli, J.W. Ochterski, P.Y. Ayala, K. Morokuma, G.A. Voth, P. Salvador, J.J. Dannenberg, V.G. Zakrzewski, S. Dapprich, A.D. Daniels, M.C. Strain, O. Farkas, D.K. Malick, A.D. Rabuck, K. Raghavachari, J.B. Foresman, J.V. Ortiz, Q. Cui, A.G. Baboul, S. Clifford, J. Cioslowski, B.B. Stefanov, G. Liu, A. Liashenko, P. Piskorz, I. Komaromi, R.L. Martin, D.J. Fox, T. Keith, M.A. Al-Laham, C.Y. Peng, A. Nanayakkara, M. Challacombe, P.M.W. Gill, B. Johnson, W. Chen, M.W. Wong, C. Gonzalez, J.A. Pople, Gaussian 03, Pittsburgh, PA, 2003.
[15] R. Schurhammer, P. Vayssiere, G. Wipff, J. Phys. Chem. A 107 (2003) 11128–11138.
[16] T.D. Vaden, C.J. Weinheimer, J.M. Lisy, J. Chem. Phys. 121 (2004) 3102–3107.
[17] T. Shimanouchi: Tables of Molecular Vibrational Frequencies, Vol. I, NIST Chemistry WebBook, NIST Standard Reference Database Number 69, National Institute of Standards and Technology, Gaithersburg, MD, http://webbook.nist.gov, accessed: June 2007 1972.
[18] D.J. Miller, J.M. Lisy, J. Am. Chem. Soc. 130 (2008) 15381–15392.
[19] R. Kusaka, Y. Inokuchi, T. Ebata, Phys. Chem. Chem. Phys. 9 (2007) 4452–4459.
[20] R. Kusaka, Y. Inokuchi, T. Ebata, Phys. Chem. Chem. Phys. 10 (2008) 6238–6244.